

## Self-Organizing Properties of Natural and Related Synthetic Glycolipids

Fabienne Dumoulin, Dominique Lafont, Paul Boullanger,\* Grahame Mackenzie,†  
Georg H. Mehl, and John W. Goodby\*

Contribution from Universite Lyon 1, Chimie Physique Electronique de Lyon,  
43 Bd du 11 Novembre 1918, F-69622 Villeurbanne, France, and The Department of Chemistry,  
The University of Hull, Hull, HU6 7RX, U.K.

Received March 18, 2002

**Abstract:** In this article we report on the syntheses, self-organizing properties, and structures of a variety of cerebrosides and related synthetic glycolipids. The thermotropic and lyotropic liquid crystalline properties of the materials were evaluated in detail. All of the families of materials studied exhibited columnar mesophases. In the dry state the aliphatic chains were found to be located on the exterior of the columns, whereas in the wet state the reverse was the case with the polar headgroups on the exterior. Thus, the aliphatic chains act almost like hydrocarbon solvents in the dry state.

### Introduction

Glycolipids are a particularly important class of cell membrane components. Principally they are only found in the exterior of cell walls, where they are typically involved in intercellular recognition processes. Cerebrosides, globosides, and gangliosides are the main classes of glycolipids which are derived from sphingosine. Sphingosine provides each of these types of glycolipid with the capacity for the attachment of two hydrocarbon chains (saturated and/or unsaturated) to the sugar headgroup, thereby allowing for molecular structures to be formed that have shapes similar to those of phospholipids, i.e. typically wedge-like, which are also prevalent in cell membranes. As the shapes of glycolipids and phospholipids are similar and as they have concomitant abilities to self-organize<sup>1</sup> in aqueous media, they easily form natural and synthetic membranes.

The number and variety of carbohydrate residues in the headgroup determine the type of glycolipid. Figure 1 shows the molecular structures of examples of derivatives of sphingosine, their prevalence in biological cell membranes, and malfunctions which are associated with them that lead to disease.<sup>2</sup> Cerebrosides, which have a single carbohydrate unit in the headgroup, are often found in nerve tissue; in cases where there is a ceramidase enzyme deficiency, there is a buildup of cerebrosides in the system, leading to diseases such as Gaucher's disease and Krabbe's disease. Gangliosides are a group of more complex glycolipids which act as specific receptors for certain pituitary glycoprotein hormones. In addition, they act as receptors for

bacterial proteins such as cholera toxin, and they behave as specific determinants for cell-cell recognition. They have an important role in the growth and differentiation of tissues, which can also lead to problems of carcinogenesis. Moreover, disorders in the assembly of gangliosides can produce hereditary diseases such as the fatal neurological Tay-Sachs disease.

Cerebrosides such as phospholipids are potentially thermotropic and lyotropic liquid crystals.<sup>3</sup> Figure 2 shows the structure of a naturally occurring cerebroside which is commercially available from Sigma.<sup>4</sup> This galactose cerebroside, which was extracted from bovine brain tissue, is a typical example of a cerebroside that is prevalent in the membranes of nerve fibers (axons). The depletion of cerebrosides through demyelination is associated with diseases such as multiple sclerosis (MS). Interestingly, some of the very earliest investigations of liquid crystals also involved the study of myelin,<sup>5</sup> and some of the textures observed in the microscope for bioactive liquid crystals have been termed myelin fingers.<sup>6</sup>

In this report we present results on the thermotropic and lyotropic liquid-crystalline self-organizing properties of naturally occurring cerebrosides **I**, their synthetic racemic dihydro analogues **II**, and related novel synthetic neoglycolipids **III** and diastereoisomers **IV** (see Chart 1). The liquid-crystalline properties of many naturally occurring and related synthetic cerebrosides, of types **I** and **II**, have been reported previously (see ref 7 and references therein). However, to provide consistency with respect to the evaluation of the physical properties of the new neoglycolipids **III**, we include comparable data measured in the same way for the three sets of materials. We have also

\* To whom correspondence should be addressed. E-mail: P.B., Paul.Boullanger@univ-lyon1.fr; J.W.G., j.w.goodby@hull.ac.uk.

† E-mail: g.mackenzie@hull.ac.uk.

(1) Blunk, D.; Praefcke, K.; Vill, V. In *Handbook of Liquid Crystals*; Demus, D., Goodby, J. W., Gray, G. W., Spiess, H.-W., Vill, V., Eds.; Wiley-VCH: Weinheim, Germany, 1998; Vol. 3 (High Molecular Weight Liquid Crystals) pp 305–340, and references therein.  
(2) Small, D. M. *J. Colloid Interface Sci.* **1977**, *58*, 581.

(3) Koynova, R.; Caffrey, M. *Biochim. Biophys. Acta* **1995**, *1255*, 213.

(4) Sigma Biochemicals and Reagents for Life Science Research.

(5) Brown, G. H.; Wolken J. J. In *Liquid Crystals and Biological Structures*; Academic Press: New York, 1979.

(6) Chapman, D. In *Liquid Crystals and Plastic Crystals*; Gray, G. W., Winsor, P. A., Eds.; Ellis Horwood: London, 1974; Vol. 1, pp 310–312.

(7) Goodby, J. W. *Liq. Cryst.* **1998**, *24*, 25.

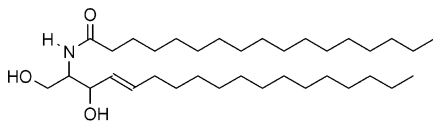
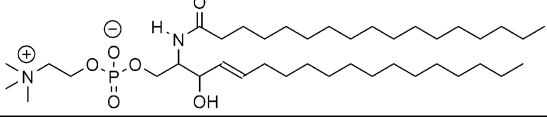
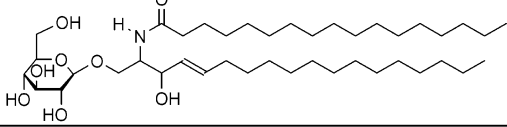
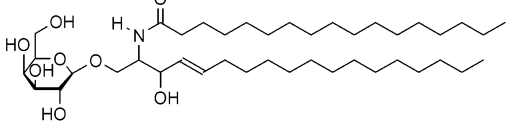
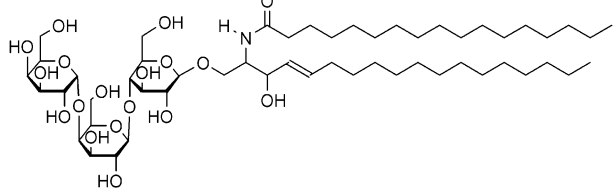
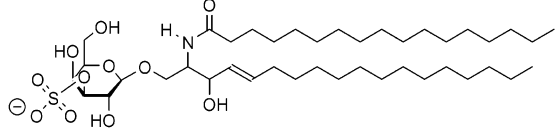
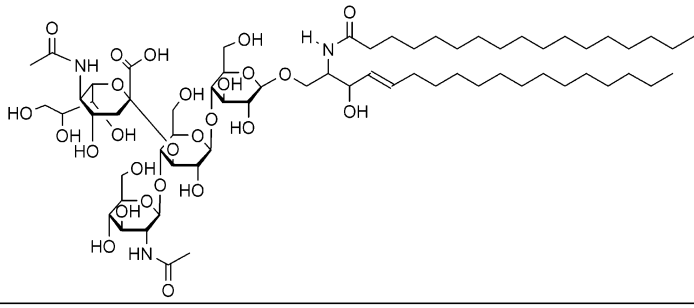
Compound Structural Class	Biological Use	Disease
	Ceramide Involved in sphingolipid metabolism	Farber's Disease
	Sphingomyelin Major component of membranes	Niemann-Pick Disease
	Glucose Cerebroside Component of nervous tissue	Gaucher's Disease
	Galactose Cerebroside Component of nervous tissue	Krabbe's Disease
	Globoside-3 Minor component of tissue	Fabry's Disease
	Galactose Cerebroside Sulphate Minor component of tissue	Metachromatic Leucodystrophy
	Gangliosides eg GM2 Minor components of many tissues	Tay-Sachs Disease

Figure 1. Sphingosine derivatives and glycolipids based on sphingosine which are found in cell membranes.

investigated the affects of chirality on mesophase formation through the synthesis and study of neoglycolipids **IV**, where chirality has been built into the branching point of the two fatty chains.

### Experimental Section

The naturally occurring cerebroside of structural type **I** and the racemic dihydro analogues **II** were purchased from Sigma and used without further purification.

**Synthetic Strategy.** The related neoglycolipids **III** were prepared via the synthetic pathways shown in Scheme 1; the synthesis of neoglycolipids **IV** has been reported elsewhere.<sup>8</sup>

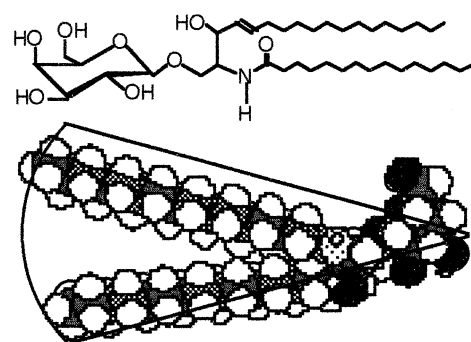
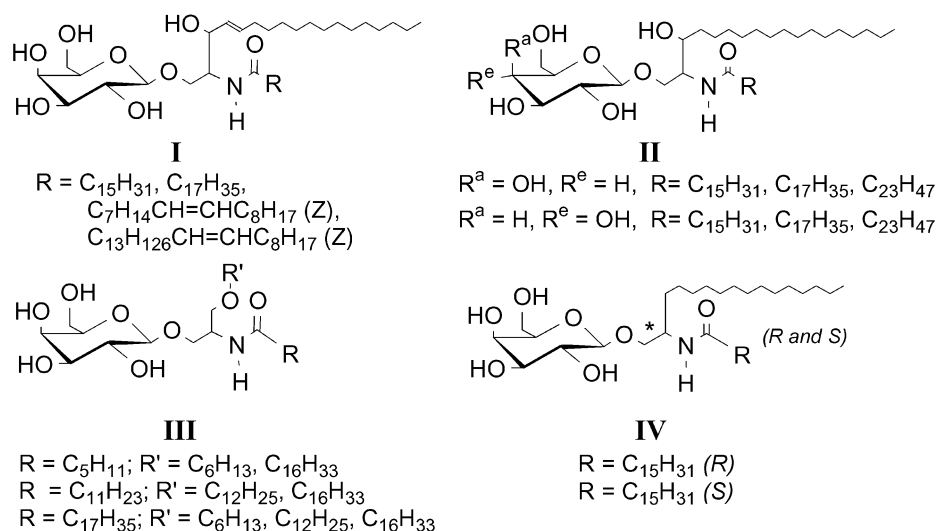
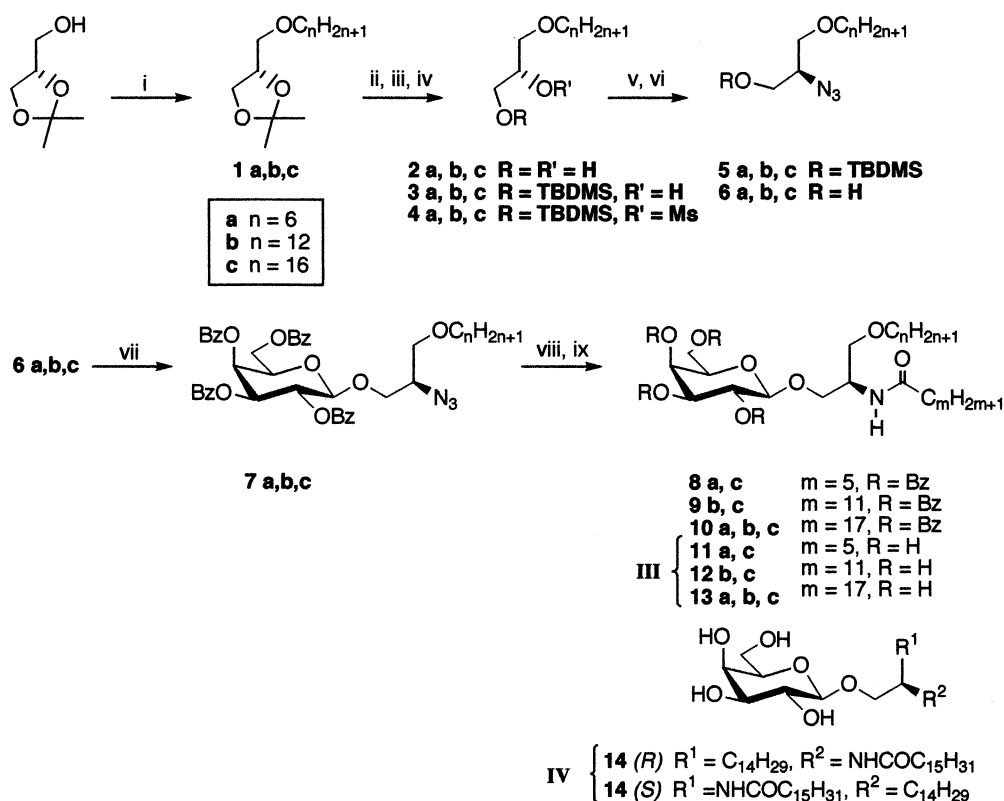


Figure 2. Wedge-like shape of naturally occurring galactocerebroside derived from bovine brain.

(8) Lafont, D.; Bouchu, M.-N.; Girard-Egrot, A.; Boullanger, P. *Carbohydr. Res.* **2001**, *336*, 181.

Chart 1

Scheme 1<sup>a</sup>

<sup>a</sup> Conditions: (i)  $C_nH_{2n+1}Br$ , 50% NaOH,  $Bu_4NBBr$ ; (ii) 80% AcOH; (iii) TBDMSCl,  $Et_3N$ , DMAP,  $CH_2Cl_2$ ; (iv) MsCl, py; (v)  $NaN_3$ , DMF; (vi)  $Bu_4NF$ , THF; (vii) 2,3,4,6-tetra-*O*-benzyl- $\alpha$ -D-galactopyranosyltrichloroacetamide, TMSOTf,  $CH_2Cl_2$ ; (viii)  $ClCOC_mH_{2m+1}$ ,  $PPh_3$ , benzene; (ix) Na catalyst, MeOH or MeOH- $CHCl_3$  (1:1).

**Neoglycolipid Synthesis.** 1,2-*O*-Isopropylidene-*sn*-glycerol was treated with an excess of *n*-hexyl, *n*-dodecyl, or *n*-hexadecyl bromide under phase-transfer conditions (50% aqueous NaOH, tetrabutylammonium bromide) at 80 °C;<sup>9</sup> compounds **1a–c** (Scheme 1) were obtained in yields from 80% to 99%. The isopropylidene acetals were cleaved in the usual manner (80% aqueous AcOH, room temperature)<sup>10</sup> to afford the diols **2a–c** in almost quantitative yields. The latter were selectively protected at the primary positions with *tert*-butyldimethylsilyl chloride in the presence of triethylamine and a catalytic amount of

4-(dimethylamino)pyridine in dichloromethane to give **3a–c** in 79–85% yields.<sup>11</sup> This procedure afforded a significantly better regioselectivity toward the primary position than the usual protocol using imidazole, as the base, in dimethylformamide.<sup>12</sup> The secondary position was then activated as a mesylate with mesyl chloride in pyridine at room temperature to afford **4a–c** in 83–88% yield; the leaving group was then displaced by nucleophilic substitution with sodium azide in dimethylformamide at 100 °C.<sup>13</sup> The substitution was confirmed by IR spectroscopy ( $\nu(N_3)$  2100  $cm^{-1}$ ). The expected azido compounds

(9) Nougier, R.; Mchich, M.; Maldonado, P.; Grangette, H. *Bull. Soc. Chim. Fr.* **1985**, *4*, 602.  
 (10) Lewbart, M. L.; Schneider, J. J. *J. Org. Chem.* **1969**, *34*, 3505.

(11) Chaudary, S. K.; Hernandez, O. *Tetrahedron Lett.* **1979**, 99.  
 (12) Corey, E. J.; Venkateswarlu, A. *J. Am. Chem. Soc.* **1972**, *94*, 6190.  
 (13) Keck, G. E.; Enholm, E. J. *J. Org. Chem.* **1985**, *50*, 146.

**5a–c** (82–88% yields) were sometimes accompanied by desilylation products (<10%). The enantiomeric purities of the azido derivatives **5a–c** were verified by  $^{19}\text{F}$  NMR, after transformation to Mosher's esters.<sup>14</sup> After desilylation in the usual manner (tetrabutylammonium fluoride in THF),<sup>12</sup> compounds **6a–c** (83–96% yields) were glycosylated before the introduction of the amido function at the secondary position of glycerol, since it has been demonstrated, in the synthesis of ceramide analogues, that the amido function deactivated the hydroxyl group in related glycosylation reactions.<sup>15</sup> The galactosylation was best effected, in our hands, with a benzoyl-protected donor, rather than an acetyl donor, with a trichloroacetimidoyl leaving group, and a catalytic amount of trimethylsilyl triflate as the promoter,<sup>16</sup> at 0 °C in dichloromethane. Nevertheless, in all cases when the 1,2-trans stereoselectivity was observed for all three acceptors, the yields varied from 47% to 88%. The amido function was then introduced by a modified Staudinger procedure that we have used previously to prepare several long-chain amido sugars.<sup>17</sup> The condensation of *n*-hexanoyl, *n*-dodecanoyl, and *n*-octadecanoyl chloride with the azido derivatives **7a–c**, in the presence of triphenylphosphine, in benzene at room temperature afforded compounds **8a,c**, **9b,c**, and **10a–c**, respectively, in 40–58% yield. These conversions were obtained without transient reduction of the azide to amine, which could in turn result in migration to give byproducts. The protected glycosides were then deprotected by Zemplén conditions, using either methanol or a 1:1 mixture of chloroform and methanol,<sup>18</sup> depending on their solubilities to afford the expected compounds **11a,c**, **12b,c**, and **13a–c** in yields from 70% to 89%.

**Experimental Procedures. General Methods.** Pyridine was dried by boiling with  $\text{CaH}_2$  prior to distillation. Dichloromethane was washed twice with water, dried over  $\text{CaCl}_2$ , and distilled from  $\text{CaH}_2$ , methanol was distilled from magnesium, tetrahydrofuran was distilled from sodium–benzophenone, and petroleum ether was distilled prior to use (bp 40–60 °C) and stored over 4 Å molecular sieves. Pyridine, THF, and  $\text{CH}_2\text{Cl}_2$  were also stored over 4 Å molecular sieves; MeOH was stored over 3 Å molecular sieves. Melting points were determined using a Büchi apparatus and were uncorrected. Thin-layer chromatography was performed on aluminum sheets coated with silica gel 60 F<sub>254</sub> (E. Merck). Compounds were visualized by spraying the TLC plates with dilute 15% aqueous  $\text{H}_2\text{SO}_4$ , followed by charring at 150 °C for a few minutes. Column chromatography was performed on silica gel Geduran Si 60 (Merck). Optical rotations were recorded on a Perkin-Elmer 241 polarimeter in a 1 dm cell at 21 °C.  $^1\text{H}$  and  $^{13}\text{C}$  NMR spectra were recorded with a Bruker AC-200 or Bruker DRX 500 spectrometer with  $\text{Me}_4\text{Si}$  ( $^1\text{H}$ ) or  $\text{CDCl}_3$  ( $^{13}\text{C}$ ,  $\delta$  77.05 ppm) as internal standard; primed signals refer to the galactopyranose ring, when present in a molecule (e.g. C-1'), whereas other signals refer to the glycerol moiety (e.g. H-2). Elemental analyses were performed by the "Laboratoire Central d'Analyses du CNRS" (Vernaison, France).

**General Procedure for the Synthesis of Compounds 1a–c.** 1,2-*O*-Isopropylidene-*sn*-glycerol<sup>19</sup> (13.2 g, 0.1 mol) was added to a 50% aqueous solution of NaOH (200 mL). The reaction mixture was heated at 80 °C, before the addition of the *n*-alkyl bromide (0.4 mol) and  $\text{Bu}_4\text{NBr}$  (6.7 g, 0.02 mol). After disappearance of the starting materials (20 h), the reaction mixture was cooled and extracted with  $\text{CH}_2\text{Cl}_2$ . The organic solution was washed twice with water, dried ( $\text{Na}_2\text{SO}_4$ ), and evaporated to dryness in vacuo. The resulting residue was subjected to chromatography over silica gel (petroleum ether, then 25:1 petroleum ether/ethyl acetate) to give the expected compound.

**3-*O*-Hexyl-1,2-*O*-isopropylidene-*sn*-glycerol (1a):**<sup>20</sup> colorless liq-

uid; 17.3 g (80%);  $[\alpha]_{\text{D}} = +18.3^\circ$  (*c* 1.2,  $\text{CHCl}_3$ );  $^1\text{H}$  NMR ( $\text{CDCl}_3$ )  $\delta$  4.26 (m, 1H, H-2), 4.06 (dd, 1H, H-1a), 3.73 (dd, 1H, H-1b), 3.56–3.37 (m, 4H, H-3a, H-3b,  $\text{OCH}_2$ ), 1.58 (t, 2H,  $\text{OCH}_2\text{CH}_2$ ), 1.43 (s, 3H,  $\text{CH}_3$ ), 1.37 (s, 3H,  $\text{CH}_3$ ), 1.26 (s, 6H, 3  $\text{CH}_2$ ), 0.88 (t, 3H,  $\text{CH}_2\text{CH}_3$ );  $^{13}\text{C}$  NMR ( $\text{CDCl}_3$ )  $\delta$  109.00 ( $\text{C}(\text{CH}_3)_2$ ), 74.60 (C-2), 71.67, 71.60 (C-3,  $\text{OCH}_2$ ), 66.79 (C-1), 25.63, 25.24 (2  $\text{CH}_3$ ), 31.54–22.46 ( $\text{OCH}_2(\text{CH}_2)_4$ ), 14.83 ( $\text{CH}_2\text{CH}_3$ ).

**3-*O*-Dodecyl-1,2-*O*-isopropylidene-*sn*-glycerol (1b):** colorless liquid; 27.0 g (90%);  $[\alpha]_{\text{D}} = +10.2^\circ$  (*c* 1.0,  $\text{CHCl}_3$ );  $^1\text{H}$  and  $^{13}\text{C}$  NMR chemical shifts are identical with those of compound **1a**  $\pm 0.05$  and  $\pm 0.1$  ppm, respectively. Anal. Calcd for  $\text{C}_{18}\text{H}_{36}\text{O}_3$ : C, 71.95; H, 12.08. Found: C, 71.89; H, 12.10.

**3-*O*-Hexadecyl-1,2-*O*-isopropylidene-*sn*-glycerol (1c):** colorless liquid; 35.5 g (99%);  $[\alpha]_{\text{D}} = +7.9^\circ$  (*c* 13.5,  $\text{CHCl}_3$ );  $^1\text{H}$  and  $^{13}\text{C}$  NMR chemical shifts are identical with those of compound **1a**  $\pm 0.06$  and  $\pm 0.7$  ppm, respectively. Anal. Calcd for  $\text{C}_{22}\text{H}_{44}\text{O}_3$ : C, 74.10; H, 12.44. Found: C, 74.20; H, 12.50.

**General Procedure for the Synthesis of Compounds 2a–c.** The acetal **1** was dissolved in 80% aqueous AcOH (1 mmol/5 mL). The mixture was stirred overnight at room temperature and then evaporated to dryness in vacuo to give an analytically pure sample.

**3-*O*-Hexyl-*sn*-glycerol (2a):**<sup>20</sup> colorless liquid; 14.2 g, (99%);  $[\alpha]_{\text{D}} = -1.5^\circ$  (*c* 1.2,  $\text{CHCl}_3$ );  $^1\text{H}$  NMR ( $\text{CDCl}_3$ )  $\delta$  3.89 (m, 1H, H-2), 3.75 (m, 2H, H-1a, H-1b), 3.53–3.36 (m, 4H, H-3a, H-3b,  $\text{OCH}_2$ ), 2.74 (bs, 1H, OH-2), 2.08 (t, 1H, OH-1), 1.54 (t, 2H,  $\text{OCH}_2\text{CH}_2$ ), 1.26 (s, 6H, 3  $\text{CH}_2$ ), 0.88 (t, 3H,  $\text{CH}_3$ );  $^{13}\text{C}$  NMR ( $\text{CDCl}_3$ )  $\delta$  72.15 (C-2), 71.76, 70.82 (C-3,  $\text{OCH}_2$ ), 64.06 (C-1), 31.65–22.57 ( $\text{OCH}_2(\text{CH}_2)_4$ ), 13.98 ( $\text{CH}_3$ ).

**3-*O*-Dodecyl-*sn*-glycerol (2b):** white powder; 23.5 g (99%); mp 50–51 °C (49–50 °C<sup>21</sup>);  $[\alpha]_{\text{D}} = -1.1^\circ$  (*c* 1.0,  $\text{CHCl}_3$ );  $^1\text{H}$  and  $^{13}\text{C}$  NMR chemical shifts are identical with those of compound **2a**  $\pm 0.05$  and  $\pm 0.4$  ppm, respectively. Anal. Calcd for  $\text{C}_{15}\text{H}_{32}\text{O}_3$ : C, 69.18; H, 12.38. Found: C, 69.36; H, 12.32.

**3-*O*-Hexadecyl-*sn*-glycerol (2c):** white powder; 31.5 g (99%); mp 64–66 °C;  $[\alpha]_{\text{D}} = -2.7^\circ$  (*c* 1.1,  $\text{CHCl}_3$ );  $^1\text{H}$  and  $^{13}\text{C}$  NMR chemical shifts are identical with those of compound **2a**  $\pm 0.07$  and  $\pm 0.3$  ppm, respectively. Anal. Calcd for  $\text{C}_{19}\text{H}_{40}\text{O}_3$ : C, 72.10; H, 12.74. Found: C, 71.87; H, 12.85.

**General Procedure for the Synthesis of Compounds 3a–c.** A solution of *tert*-butyldimethylsilyl chloride (1.4 equiv) in dichloromethane (1 mmol/mL) was added dropwise to a solution of the diol **2** in dichloromethane (1 equiv, 1 mmol/mL), containing triethylamine (1.4 equiv) and (dimethylamino)pyridine (0.06 equiv). After disappearance of the diol **2** (18 h at room temperature), the reaction mixture was washed twice with water and the aqueous phase was back-extracted with dichloromethane. The organic phases were combined, the solvent was removed in vacuo, and the subsequent residue was purified via silica gel column chromatography (6:1 petroleum ether/ethyl acetate).

**1-*O*-(*tert*-Butyldimethylsilyl)-3-*O*-hexyl-*sn*-glycerol (3a):** colorless liquid; 19.7 g (85%);  $[\alpha]_{\text{D}} = +36.9^\circ$  (*c* 1.0,  $\text{CHCl}_3$ );  $^1\text{H}$  NMR ( $\text{CDCl}_3$ )  $\delta$  3.80 (m, 1H, H-2), 3.65 (dd, 2H, H-1a, H-1b), 3.46 (m, 4H, H-3a, H-3b,  $\text{OCH}_2$ ), 2.50 (t, 1H, OH-2), 1.60 (bs, 2H,  $\text{OCH}_2\text{CH}_2$ ), 1.26 (s, 6H, 3  $\text{CH}_2$ ), 0.89 (t, 12H, 4  $\text{CH}_3$ ), 0.08 (s, 6H, 2  $\text{CH}_3\text{Si}$ );  $^{13}\text{C}$  NMR ( $\text{CDCl}_3$ )  $\delta$  71.67, 71.49 (C-3,  $\text{OCH}_2$ ), 70.65 (C-2), 64.10 (C-1), 31.69–22.62 ( $\text{OCH}_2(\text{CH}_2)_4$ ), 25.80, 25.88 ( $\text{C}(\text{CH}_3)_3$ ), 18.28 ( $\text{C}(\text{CH}_3)_3$ ), 14.03 ( $\text{CH}_3$ ), –5.43 ( $\text{Si}(\text{CH}_3)_2$ ). Anal. Calcd for  $\text{C}_{15}\text{H}_{34}\text{O}_3\text{Si}$ : C, 62.01; H, 11.80. Found: C, 62.06; H, 11.70.

**1-*O*-(*tert*-Butyldimethylsilyl)-3-*O*-dodecyl-*sn*-glycerol (3b):** colorless liquid; 27.0 g (80%);  $[\alpha]_{\text{D}} = +16.2^\circ$  (*c* 1.3,  $\text{CHCl}_3$ );  $^1\text{H}$  and  $^{13}\text{C}$  NMR chemical shifts are identical with those of compound **3a**  $\pm 0.04$  and  $\pm 0.1$  ppm, respectively. Anal. Calcd for  $\text{C}_{21}\text{H}_{46}\text{O}_3\text{Si}$ : C, 67.32; H, 12.37. Found: C, 67.22; H, 12.19.

(21) Hong, C. I.; Nechaev, A.; Kirisits, A. J.; Vigs, R.; Hui, S.-W.; West, C. R. *J. Med. Chem.* **1995**, *38*, 1629.

(14) Dale, J. A.; Dull, D. L.; Mosher, H. S. *J. Org. Chem.* **1969**, *34*, 2543.  
(15) Schmidt, R. R.; Zimmermann, P. *Angew. Chem., Int. Ed. Engl.* **1986**, *25*, 725.

(16) Rio, S.; Beau, J.-M.; Jacquinet, J.-C. *Carbohydr. Res.* **1991**, *219*, 71.

(17) Boullanger, P.; Maunier, V.; Lafont, D. *Carbohydr. Res.* **2000**, *324*, 97.

(18) Reinhard, B.; Faillard, H. *Liebigs Ann. Chem.* **1994**, 193.

(19) Takano, S.; Goto, E.; Hirama, M.; Ogasawara, K. *Heterocycles* **1981**, *16*, 381.

(20) Wheeler, T. N.; Blanchard, S. G.; Andrews, R. C.; Fang, F.; Gray-Nunez, Y. *J. Med. Chem.* **1994**, *37*, 4118.

**1-*O*-(*tert*-Butyldimethylsilyl)-3-*O*-hexadecyl-*sn*-glycerol (3c):** colorless liquid; 33.9 g (79%);  $[\alpha]_D = -3.7^\circ$  (*c* 1.4, CH<sub>3</sub>OH); <sup>1</sup>H and <sup>13</sup>C NMR chemical shifts are identical with those of compound **3a**  $\pm 0.03$  and  $\pm 0.1$  ppm, respectively. Anal. Calcd for C<sub>25</sub>H<sub>54</sub>O<sub>3</sub>Si: C, 69.70; H, 12.64. Found: C, 69.88; H, 12.48.

**General Procedure for the Synthesis of Compounds 4a–c.** Mesyl chloride (2 equiv) was added dropwise to a stirred solution of the monosilyl derivative **3** in pyridine (1 equiv, 1 mmol/2 mL) at 0 °C. The reaction mixture was allowed to reach room temperature, stirred overnight, and then taken to dryness. The residue was diluted with ethyl acetate and washed sequentially with saturated solutions of sodium bicarbonate and sodium chloride. The organic phase was dried (Na<sub>2</sub>SO<sub>4</sub>), the solvent removed in vacuo, and the subsequent residue purified by silica gel chromatography (5:1 petroleum ether/ethyl acetate) to give the expected product.

**1-*O*-(*tert*-Butyldimethylsilyl)-3-*O*-hexyl-2-*O*-mesyl-*sn*-glycerol (4a):** colorless oil; 22.0 g (88%);  $[\alpha]_D = -3.1^\circ$  (*c* 1.0, CHCl<sub>3</sub>); <sup>1</sup>H NMR (CDCl<sub>3</sub>)  $\delta$  4.75 (m, 1H, H-2), 3.85 (d, 2H, H-1a, H-1b), 3.65 (d, 2H, H-3a, H-3b), 3.45 (t, 2H, OCH<sub>2</sub>), 3.07 (s, 3H, SCH<sub>3</sub>), 1.65 (t, 2H, OCH<sub>2</sub>CH<sub>2</sub>), 1.30 (s, 6H, 3 CH<sub>2</sub>), 0.90 (t, 12H, 4 CH<sub>3</sub>), 0.15 (s, 6H, 2 CH<sub>3</sub>Si); <sup>13</sup>C NMR (CDCl<sub>3</sub>)  $\delta$  82.09 (C-2), 69.75, 71.78 (C-3, OCH<sub>2</sub>), 62.77 (C-1), 38.77 (SCH<sub>3</sub>), 31.64–25.97 (OCH<sub>2</sub>(CH<sub>2</sub>)<sub>4</sub>), 25.85 (C(CH<sub>3</sub>)<sub>3</sub>), 18.28 (C(CH<sub>3</sub>)<sub>3</sub>), 14.16 (CH<sub>3</sub>), –5.48, –5.46 (SiCH<sub>3</sub>). Anal. Calcd for C<sub>16</sub>H<sub>36</sub>O<sub>5</sub>SSi: C, 52.20; H, 9.86; S, 8.71. Found: C, 52.15; H, 9.74; S, 8.78.

**1-*O*-(*tert*-Butyldimethylsilyl)-3-*O*-dodecyl-2-*O*-mesyl-*sn*-glycerol (4b):** colorless oil; 27.1 g (83%);  $[\alpha]_D = -6.6^\circ$  (*c* 1.1, CHCl<sub>3</sub>); <sup>1</sup>H and <sup>13</sup>C NMR chemical shifts are identical with those of compound **4a**  $\pm 0.04$  and  $\pm 0.06$  ppm, respectively. Anal. Calcd for C<sub>22</sub>H<sub>48</sub>O<sub>5</sub>SSi: C, 58.36; H, 10.68; S, 7.08. Found: C, 58.08; H, 10.69; S, 7.31.

**1-*O*-(*tert*-Butyldimethylsilyl)-3-*O*-hexadecyl-2-*O*-mesyl-*sn*-glycerol (4c):** colorless oil; 34.0 g (85%);  $[\alpha]_D = -6.2^\circ$  (*c* 1.6, CHCl<sub>3</sub>); <sup>1</sup>H and <sup>13</sup>C NMR chemical shifts are identical with those of compound **4a**  $\pm 0.07$  and  $\pm 0.07$  ppm, respectively. Anal. Calcd for C<sub>26</sub>H<sub>56</sub>O<sub>5</sub>SSi: C, 61.40; H, 11.10; S, 6.30. Found: C, 61.57; H, 11.08; S, 5.99.

**General Procedure for the Synthesis of Compounds 5a–c.** Sodium azide (5 equiv) was added to a solution of **4** in DMF (1 equiv, 1 mmol/7 mL). The mixture was heated at 100 °C for 14 h and the solvent removed in vacuo. The residue was diluted with dichloromethane and washed sequentially with water and saturated solutions of sodium bicarbonate and sodium chloride. The organic phase was separated and dried (Na<sub>2</sub>SO<sub>4</sub>), and the solvent was removed in vacuo and the subsequent residue purified by silica gel column chromatography (15:1 petroleum ether/ethyl acetate) to give the expected product.

**2-Azido-3-*O*-(*tert*-butyldimethylsilyl)-2-deoxy-1-*O*-hexyl-*sn*-glycerol (5a):** colorless oil; 15.2 g (82%);  $[\alpha]_D = +2.5^\circ$  (*c* 1.3, CHCl<sub>3</sub>); <sup>1</sup>H NMR (CDCl<sub>3</sub>)  $\delta$  3.75 (dd, 2H, H-3a, H-3b), 3.55 (m, 3H, H-2, H-1a, H-1b), 3.45 (t, 2H, OCH<sub>2</sub>), 1.65 (t, 2H, OCH<sub>2</sub>CH<sub>2</sub>), 1.38 (s, 6H, 3 CH<sub>2</sub>), 1.00 (t, 12H, 4 CH<sub>3</sub>), 0.15 (s, 6H, 2 CH<sub>3</sub>Si); <sup>13</sup>C NMR (CDCl<sub>3</sub>)  $\delta$  69.84, 71.75 (C-1, OCH<sub>2</sub>), 63.31 (C-3), 62.35 (C-2), 31.68–25.76 (OCH<sub>2</sub>(CH<sub>2</sub>)<sub>4</sub>), 25.82 (C(CH<sub>3</sub>)<sub>3</sub>), 18.27 (C(CH<sub>3</sub>)<sub>3</sub>), 14.06 (CH<sub>3</sub>), –5.51 (Si(CH<sub>3</sub>)<sub>2</sub>). Anal. Calcd for C<sub>15</sub>H<sub>33</sub>N<sub>3</sub>O<sub>2</sub>Si: C, 57.28; H, 10.58; N, 13.36. Found: C, 57.32; H, 10.58; N, 13.36.

**2-Azido-3-*O*-(*tert*-butyldimethylsilyl)-2-deoxy-1-*O*-dodecyl-*sn*-glycerol (5b):** colorless oil; 19.8 g (84%);  $[\alpha]_D = +4.6^\circ$  (*c* 0.7, CHCl<sub>3</sub>); <sup>1</sup>H and <sup>13</sup>C NMR chemical shifts are identical with those of compound **5a**  $\pm 0.03$  and  $\pm 0.06$  ppm, respectively. Anal. Calcd for C<sub>21</sub>H<sub>45</sub>N<sub>3</sub>O<sub>2</sub>Si: C, 63.10; H, 11.35; N, 10.51. Found: C, 63.38; H, 11.15; N, 10.22.

**2-Azido-3-*O*-(*tert*-butyldimethylsilyl)-2-deoxy-1-*O*-hexadecyl-*sn*-glycerol (5c):** colorless oil; 22.0 g (88%);  $[\alpha]_D = +3.3^\circ$  (*c* 1.0, CHCl<sub>3</sub>); <sup>1</sup>H and <sup>13</sup>C NMR chemical shifts are identical with those of compound **5a**  $\pm 0.04$  and  $\pm 0.01$  ppm, respectively. Anal. Calcd for C<sub>25</sub>H<sub>53</sub>N<sub>3</sub>O<sub>2</sub>Si: C, 65.88; H, 11.72; N, 9.22. Found: C, 65.58; H, 11.55; N, 9.30.

**General Procedure for the Synthesis of Compounds 6a–c.** Tetrabutylammonium fluoride (3 equiv) was added to a solution of the silyl product **5** in THF (1 equiv, 1 mmol/5 mL), and the reaction mixture

was stirred for 1.5 h at room temperature. The reaction mixture was evaporated to dryness, the residue was diluted with dichloromethane, and this solution was sequentially washed with saturated solutions of sodium bicarbonate and sodium chloride. The aqueous phases were back-extracted with dichloromethane. The organic phases were combined and dried (Na<sub>2</sub>SO<sub>4</sub>), and the solvent was removed in vacuo to give a residue which was purified by silica gel column chromatography (1:1 petroleum ether/ethyl acetate) to give the expected product.

**2-Azido-2-deoxy-1-*O*-hexyl-*sn*-glycerol (6a):** colorless oil; 8.2 g (83%);  $[\alpha]_D = -8.2^\circ$  (*c* 1.8, CHCl<sub>3</sub>); <sup>1</sup>H NMR (CDCl<sub>3</sub>)  $\delta$  3.68 (m, 5H, H-1a, H-1b, H-2, H-3a, H-3b), 3.48 (t, 2H, OCH<sub>2</sub>), 2.15 (t, 1H, OH-3), 1.68 (t, 2H, OCH<sub>2</sub>CH<sub>2</sub>), 1.35 (s, 6H, 3 CH<sub>2</sub>), 0.95 (t, 3H, CH<sub>3</sub>); <sup>13</sup>C NMR (CDCl<sub>3</sub>)  $\delta$  71.03, 71.95 (C-1, OCH<sub>2</sub>), 63.09 (C-3), 62.30 (C-2), 31.65–25.69 (OCH<sub>2</sub>(CH<sub>2</sub>)<sub>4</sub>), 14.06 (CH<sub>3</sub>). Anal. Calcd for C<sub>9</sub>H<sub>19</sub>N<sub>3</sub>O<sub>2</sub>: C, 53.71; H, 9.51; N, 20.88. Found: C, 54.05; H, 9.73; N, 20.68.

**2-Azido-2-deoxy-1-*O*-dodecyl-*sn*-glycerol (6b):** colorless oil; 13.6 g (96%);  $[\alpha]_D = -17.1^\circ$  (*c* 2.4, CHCl<sub>3</sub>); <sup>1</sup>H and <sup>13</sup>C NMR chemical shifts are identical with those of compound **6a**  $\pm 0.04$  and  $\pm 0.3$  ppm, respectively. Anal. Calcd for C<sub>15</sub>H<sub>31</sub>N<sub>3</sub>O<sub>2</sub>: C, 63.12; H, 10.95; N, 14.72. Found: C, 63.22; H, 11.00; N, 14.49.

**2-Azido-2-deoxy-1-*O*-hexadecyl-*sn*-glycerol (6c):** white amorphous solid; 14.5 g (88%);  $[\alpha]_D = -10.5^\circ$  (*c* 1.8, CHCl<sub>3</sub>); <sup>1</sup>H and <sup>13</sup>C NMR chemical shifts are identical with those of compound **6a**  $\pm 0.07$  and  $\pm 0.3$  ppm, respectively. Anal. Calcd for C<sub>19</sub>H<sub>39</sub>N<sub>3</sub>O<sub>2</sub>: C, 66.81; H, 11.51; N, 12.30. Found: C, 66.75; H, 11.52; N, 12.20.

**General Procedure for the Synthesis of Compounds 7a–c.** A solution of 2,3,4,6-tetra-*O*-benzoyl- $\alpha$ -D-galactopyranosyl trichloroacetimidate<sup>16</sup> (1 equiv, 1 mmol/12 mL) and the azide **6** (1 equiv) in freshly distilled dichloromethane was stirred at 0 °C under argon in the presence of mashed 4 Å molecular sieves. A 10% solution of (trimethylsilyl)-trifluoromethane sulfonate (0.03 equiv) in dichloromethane was then added dropwise to the reaction mixture over 1 h. This mixture was stirred overnight at 0 °C, filtered through Celite, and washed twice with saturated sodium bicarbonate solution and water. The organic phase was dried (Na<sub>2</sub>SO<sub>4</sub>), and the solvent was removed in vacuo to give a residue which was purified by silica gel column chromatography (3:1 petroleum ether/ethyl acetate).

**2-Azido-3-*O*-(2,3,4,6-tetra-*O*-benzoyl- $\beta$ -D-galactopyranosyl)-2-deoxy-1-*O*-hexyl-*sn*-glycerol (7a):** colorless oil; 1.571 g (47%);  $[\alpha]_D = +76.6^\circ$  (*c* 1.0, CHCl<sub>3</sub>); <sup>1</sup>H NMR (CDCl<sub>3</sub>)  $\delta$  8.12–7.21 (m, 20 H, aromatics), 6.12 (bd, 1H, H-4', *J*<sub>3',4'</sub> = 3.2 Hz), 5.83 (dd, 1H, H-2', *J*<sub>1',2'</sub> = 7.8 Hz, *J*<sub>2',3'</sub> = 10.4 Hz), 5.57 (dd, 1H, H-3'), 4.87 (d, 1H, H-1'), 4.71 (dd, 1H, H-6'a, *J*<sub>5,6'a</sub> = 6.2 Hz, *J*<sub>6'a,6'b</sub> = 10.8 Hz), 4.48–4.31 (m, 2H, H-5', H-6'a), 4.02 (m, 1H, H-3a), 3.71 (m, 2H, H-3b, H-2), 3.37–3.56 (m, 2H, OCH<sub>2</sub>CH<sub>2</sub>), 3.28–3.10 (m, 2H, H-1a, H-1b), 1.44 (bs, 2H, OCH<sub>2</sub>CH<sub>2</sub>), 1.26 (bs, 6H, 3 CH<sub>2</sub>), 0.88 (t, 3H, CH<sub>3</sub>); <sup>13</sup>C NMR (CDCl<sub>3</sub>)  $\delta$  166.06, 165.63, 165.60, 165.31 (C=O), 133.69, 133.37 (C<sup>IV</sup>, aromatics), 130.06, 129.82, 129.51, 129.42, 129.11, 128.86, 128.71, 128.55, 128.49, 128.37 (CH, aromatics), 101.87 (C-1'), 71.68, 71.57 (C-3', C-5'), 71.54, 70.16 (C-1, OCH<sub>2</sub>), 69.85 (C-2'), 68.74 (C-3), 68.26 (C-4'), 62.15 (C-6'), 60.20 (C-2), 31.64–22.65 (OCH<sub>2</sub>(CH<sub>2</sub>)<sub>4</sub>), 14.13 (CH<sub>3</sub>). Anal. Calcd for C<sub>43</sub>H<sub>45</sub>N<sub>3</sub>O<sub>11</sub>: C, 66.23; H, 5.82; N, 5.39. Found: C, 66.12; H, 5.73; N, 5.18.

**2-Azido-3-*O*-(2,3,4,6-tetra-*O*-benzoyl- $\beta$ -D-galactopyranosyl)-2-deoxy-1-*O*-dodecyl-*sn*-glycerol (7b):** colorless oil; 2.535 g (88%);  $[\alpha]_D = +61.9^\circ$  (*c* 0.8, CHCl<sub>3</sub>); <sup>1</sup>H NMR chemical shifts are identical with those of compound **7a**  $\pm 0.07$  ppm (coupling constants  $\pm 0.1$  Hz), and <sup>13</sup>C chemical shifts are identical with those of compound **7a**  $\pm 0.1$  ppm. Anal. Calcd for C<sub>49</sub>H<sub>57</sub>N<sub>3</sub>O<sub>11</sub>: C, 68.12; H, 6.65; N, 4.86. Found: C, 68.30; H, 6.86; N, 4.90.

**2-Azido-3-*O*-(2,3,4,6-tetra-*O*-benzoyl- $\beta$ -D-galactopyranosyl)-2-deoxy-1-*O*-hexadecyl-*sn*-glycerol (7c):** colorless oil; 1.665 g (61%);  $[\alpha]_D = +53.7^\circ$  (*c* 2.9, CHCl<sub>3</sub>); <sup>1</sup>H NMR chemical shifts are identical with those of compound **7a**  $\pm 0.06$  ppm (coupling constants  $\pm 0.1$  Hz), and <sup>13</sup>C chemical shifts are identical with those of compound **7a**  $\pm 0.1$

ppm. Anal. Calcd for  $C_{53}H_{65}N_3O_{11}$ : C, 69.18; H, 7.12; N, 4.57. Found: C, 68.64; H, 7.24; N, 4.58.

**General Procedure for the Synthesis of Compounds 8a,c, 9b,c, and 10a–c.** The acid chloride (1.5 equiv) was added, under argon, to a stirred solution of the azide **7** (1 equiv, 1 mmol/8 mL) in freshly distilled benzene containing activated 4 Å molecular sieves (0.2 g/mL). A solution of triphenylphosphine in benzene (1.5 equiv, 1 mmol/mL) was added dropwise to the reaction mixture, which was then stirred for 48 h, at which time the reaction appeared to have reached completion by TLC. The reaction mixture was filtered through Celite and concentrated in vacuo to a gum, which was purified by silica gel column chromatography (1:1 or 2:1 petroleum ether/ethyl acetate) to give the expected product.

**3-O-(2,3,4,6-Tetra-O-benzoyl-β-D-galactopyranosyl)-2-deoxy-2-hexanamido-1-O-hexyl-sn-glycerol (8a):** obtained from **7a** and hexanoyl chloride, following the general procedure, as an amorphous solid; 621 mg (45%);  $[\alpha]_D = +42.2^\circ$  (*c* 0.8,  $CHCl_3$ );  $^1H$  NMR ( $CDCl_3$ )  $\delta$  8.21–7.31 (m, 20 H, aromatics), 5.91 (bd, 1H, H-4',  $J_{3',4'} = 3.1$  Hz), 5.72 (dd, 1H, H-2',  $J_{1',2'} = 7.6$  Hz,  $J_{2',3'} = 10.4$  Hz), 5.64 (dd, 2H, H-3', NH), 4.83 (d, 1H, H-1'), 4.61 (dd, 1H, H-6'a,  $J_{5',6'a} = 6.1$  Hz,  $J_{6'a,6'b} = 10.6$  Hz), 4.47–4.25 (m, 3H, H-2, H-5', H-6'b), 4.11 (dd, H-3a), 3.71 (dd, 1H, H-3b), 3.47–3.23 (m, 4H, H-1a, H-1b,  $OCH_2CH_2$ ), 2.31 (t, 2H,  $NHCOCH_2$ ), 1.42 (t, 2H,  $OCH_2CH_2$ ), 1.25 (bs, 12H, 6  $CH_2$ ), 0.88 (t, 6H, 2  $CH_3$ );  $^{13}C$  NMR ( $CDCl_3$ )  $\delta$  172.78 (CONH), 166.04, 165.58, 165.54, 165.35 (C=O), 133.65, 133.49, 133.32 ( $C^{IV}$ , aromatics), 130.06, 129.83, 129.80, 129.77, 129.45, 129.25, 129.10, 128.82, 128.69, 128.56, 128.50, 128.33 (CH, aromatics), 101.85 (C-1'), 71.53–71.45 (C-3', C-5'), 71.33, 68.65 (C-1,  $OCH_2$ ), 70.12 (C-2'), 68.49 (C-3), 68.14 (C-4'), 62.05 (C-6'), 48.09 (C-2), 36.49 ( $NHCOCH_2$ ), 31.97–22.40 ( $(CH_2)_n$ ), 14.18–13.99 (2  $CH_3$ ). Anal. Calcd for  $C_{49}H_{57}NO_{12}$ : C, 69.08; H, 6.74; N, 1.64. Found: C, 69.38; H, 6.80; N, 1.72.

**3-O-(2,3,4,6-Tetra-O-benzoyl-β-D-galactopyranosyl)-2-deoxy-1-O-hexadecyl-2-hexanamido-sn-glycerol (8c):** obtained from **7c** and hexanoyl chloride, following the general procedure, as an amorphous solid; 300 mg (49%);  $[\alpha]_D = +57.7^\circ$  (*c* 1.0,  $CHCl_3$ );  $^1H$  NMR chemical shifts are identical with those of compound **8a**  $\pm 0.10$  ppm (coupling constants  $\pm 0.1$  Hz), and  $^{13}C$  chemical shifts are identical with those of compound **8a**  $\pm 0.5$  ppm. Anal. Calcd for  $C_{59}H_{77}NO_{12}$ : C, 71.42; H, 7.82; N, 1.41. Found: C, 71.65; H, 8.08; N, 1.56.

**3-O-(2,3,4,6-Tetra-O-benzoyl-β-D-galactopyranosyl)-2-deoxy-2-dodecanamido-1-O-dodecyl-sn-glycerol (9b):** obtained from **7b** and dodecanoyl chloride, following the general procedure, as an amorphous solid; 700 mg (40%);  $[\alpha]_D = +50.9^\circ$  (*c* 0.8,  $CHCl_3$ );  $^1H$  NMR chemical shifts are identical with those of compound **8a**  $\pm 0.10$  ppm (coupling constants  $\pm 0.1$  Hz), and  $^{13}C$  chemical shifts are identical with those of compound **8a**  $\pm 0.5$  ppm. Anal. Calcd for  $C_{61}H_{81}NO_{12}$ : C, 71.81; H, 8.00; N, 1.37. Found: C, 71.86; H, 8.13; N, 1.44.

**3-O-(2,3,4,6-Tetra-O-benzoyl-β-D-galactopyranosyl)-2-deoxy-2-dodecanamido-1-O-hexadecyl-sn-glycerol (9c):** obtained as an amorphous solid from **7c** and dodecanoyl chloride following the general procedure; 443 mg (45%);  $[\alpha]_D = +48.4^\circ$  (*c* 0.76,  $CHCl_3$ );  $^1H$  NMR chemical shifts are identical with those of compound **8a**  $\pm 0.10$  ppm (coupling constants  $\pm 0.1$  Hz), and  $^{13}C$  chemical shifts are identical with those of compound **8a**  $\pm 0.5$  ppm. Anal. Calcd for  $C_{65}H_{89}NO_{12}$ : C, 72.53; H, 8.33; N, 1.30. Found: C, 72.29; H, 8.56; N, 1.18.

**3-O-(2,3,4,6-Tetra-O-benzoyl-β-D-galactopyranosyl)-2-deoxy-1-O-hexyl-2-octadecanamido-sn-glycerol (10a):** obtained as an amorphous solid from **7a** and octadecanoyl chloride following the general procedure; 345 mg (58%);  $[\alpha]_D = +55.5^\circ$  (*c* 0.8,  $CHCl_3$ );  $^1H$  NMR chemical shifts are identical with those of compound **8a**  $\pm 0.10$  ppm (coupling constants  $\pm 0.1$  Hz), and  $^{13}C$  chemical shifts are identical with those of compound **8a**  $\pm 0.5$  ppm. Anal. Calcd for  $C_{61}H_{81}NO_{12}$ : C, 71.81; H, 8.00; N, 1.37. Found: C, 72.03; H, 8.10; N, 1.31.

**3-O-(2,3,4,6-Tetra-O-benzoyl-β-D-galactopyranosyl)-2-deoxy-1-O-dodecyl-2-octadecanamido-sn-glycerol (10b):** obtained as an amorphous solid from **7b** and octadecanoyl chloride following the general

procedure; 678 mg (57%);  $[\alpha]_D = +49.4^\circ$  (*c* 0.8,  $CHCl_3$ );  $^1H$  NMR chemical shifts are identical with those of compound **8a**  $\pm 0.10$  ppm (coupling constants  $\pm 0.1$  Hz), and  $^{13}C$  chemical shifts are identical with those of compound **8a**  $\pm 0.5$  ppm. Anal. Calcd for  $C_{67}H_{93}NO_{12}$ : C, 72.86; H, 8.49; N, 1.27. Found: C, 73.23; H, 8.64; N, 1.45.

**3-O-(2,3,4,6-Tetra-O-benzoyl-β-D-galactopyranosyl)-2-deoxy-1-O-hexadecyl-2-octadecanamido-sn-glycerol (10c):** obtained as an amorphous solid from **7c** and octadecanoyl chloride following the general procedure; 414 mg (57%);  $[\alpha]_D = +37.4^\circ$  (*c* 0.9,  $CHCl_3$ );  $^1H$  NMR chemical shifts are identical with those of compound **8a**  $\pm 0.10$  ppm (coupling constants  $\pm 0.1$  Hz), and  $^{13}C$  chemical shifts are identical with those of compound **8a**  $\pm 0.5$  ppm. Anal. Calcd for  $C_{71}H_{101}NO_{12}$ : C, 73.48; H, 8.77; N, 1.21. Found: C, 73.14; H, 8.91; N, 1.28.

**General Procedure for the Synthesis of Compounds 11a,c, 12b,c, and 13a–c.** A catalytic amount of sodium (0.1 equiv) was dissolved in a solution of the benzoyleated compound in either methanol or 1:1 chloroform/methanol (1 equiv, 1 mmol/20 mL), and the mixture was then stirred for 18 h, at room temperature. The deprotected product was filtered and adsorbed on silica gel, and the cake was deposited at the top of a column of silica gel for chromatographic purification (8:1 dichloromethane/methanol) to give the expected product. Due to the poor solubility of the products in all normal bench solvents,  $[\alpha]_D$  values were not determined.

**2-Deoxy-3-O-β-D-galactopyranosyl-2-hexanamido-1-O-hexyl-sn-glycerol (11a):** obtained from **8a**, as a white amorphous solid; 149 mg (85%);  $^1H$  NMR ( $CDCl_3$ )  $\delta$  6.52 (bd, 1H, NH), 4.73–4.49 (2 bs, 2H, 2 OH), 4.28–2.04 (m, 18H, 2 OH, H-1', H-2', H-3', H-4', H-5', H-6a', H-6b', H-1a, H-1b, H-2, H-3a, H-3b,  $OCH_2CH_2$ ,  $NHCOCH_2$ ), 1.54 (bs, 2H,  $OCH_2CH_2$ ), 1.26 (bs, 12H, 6  $CH_2$ ), 0.88 (t, 6H, 2  $CH_3$ );  $^{13}C$  NMR ( $CDCl_3$ )  $\delta$  174.23 (C=O), 104.36 (C-1'), 74.68, 73.68 (C-3', C-5'), 71.50 (C-3), 71.21 (C-2'), 69.57, 69.10 (C-1,  $OCH_2CH_2$ ), 68.64 (C-4'), 61.06 (C-6'), 48.86 (C-2), 36.62 ( $NHCOCH_2$ ), 31.69–22.44 ( $(CH_2)_n$ ), 14.06, 14.00 (2  $CH_3$ ). Anal. Calcd for  $C_{21}H_{41}NO_8$ : C, 57.91; H, 9.49; N, 3.22. Found: C, 58.24; H, 9.87; N, 3.22.

**2-Deoxy-3-O-β-D-galactopyranosyl-1-O-hexadecyl-2-hexanamido-sn-glycerol (11c):** obtained from **8c**, as a white solid; 150 mg (78%);  $^1H$  and  $^{13}C$  NMR chemical shifts are identical with those of compound **11a**  $\pm 0.1$  and  $\pm 1.0$  ppm, respectively. Anal. Calcd for  $C_{31}H_{61}NO_8$ : C, 64.66; H, 10.69; N, 2.43. Found: C, 64.33; H, 10.80; N, 2.53.

**2-Deoxy-2-dodecanamido-1-O-dodecyl-3-O-β-D-galactopyranosyl-sn-glycerol (12b):** obtained from **9b**, as a white solid; 241 mg (89%);  $^1H$  and  $^{13}C$  NMR chemical shifts are identical with those of compound **11a**  $\pm 0.1$  and  $\pm 1.0$  ppm, respectively. Anal. Calcd for  $C_{33}H_{65}NO_8$ : C, 65.64; H, 10.85; N, 2.32. Found: C, 65.14; H, 10.73; N, 2.40.

**2-Deoxy-2-dodecanamido-3-O-β-D-galactopyranosyl-1-O-hexadecyl-sn-glycerol (12c):** obtained from **9c**, as a white solid; 228 mg (83%);  $^1H$  NMR ( $C_5D_5N$ )  $\delta$  8.48 (bd, 1H, NH), 6.79 (bs, 1H, OH), 6.52 (m, 2H, 2 OH), 4.88–2.37 (m, 17H, OH, H-1', H-2', H-3', H-4', H-5', H-6a', H-6b', H-1a, H-1b, H-2, H-3a, H-3b,  $OCH_2CH_2$ ,  $NHCOCH_2$ ), 1.54 (bs, 2H,  $OCH_2CH_2$ ), 1.27 (bs, 44H, 22  $CH_2$ ), 0.87 (t, 6H, 2  $CH_3$ );  $^{13}C$  NMR ( $C_5D_5N$ )  $\delta$  173.54 (C=O), 106.60 (C-1'), 77.30, 75.57 (C-3', C-5'), 72.89 (C-2'), 71.58 (C-3), 70.38, 70.31 (C-1,  $OCH_2CH_2$ ), 70.30 (C-4'), 62.51 (C-6'), 50.09 (C-2), 36.88 ( $NHCOCH_2$ ), 32.29–23.16 ( $(CH_2)_n$ ), 14.47 (2  $CH_3$ ). Anal. Calcd for  $C_{37}H_{73}NO_8$ : C, 67.33; H, 11.15; N, 2.12. Found: C, 66.88; H, 11.21; N, 2.39.

**2-Deoxy-3-O-β-D-galactopyranosyl-1-O-hexyl-2-octadecanamido-sn-glycerol (13a):** obtained as a white solid from **10a**; 205 mg (77%);  $^1H$  and  $^{13}C$  NMR chemical shifts are identical with those of compound **11a**  $\pm 0.1$  and  $\pm 1.0$  ppm, respectively. Anal. Calcd for  $C_{33}H_{65}NO_8$ : C, 65.64; H, 10.85; N, 2.32. Found: C, 65.54; H, 11.06; N, 2.50.

**2-Deoxy-1-O-dodecyl-3-O-β-D-galactopyranosyl-2-octadecanamido-sn-glycerol (13b):** obtained as a white solid from **10b**; 284 mg (70%);  $^1H$  and  $^{13}C$  NMR chemical shifts are identical with those of compound **12c**  $\pm 0.2$  and  $\pm 1.1$  ppm, respectively. Anal. Calcd for  $C_{39}H_{77}NO_8$ : C, 68.08; H, 11.28; N, 2.04. Found: C, 68.07; H, 11.63; N, 1.94.

**2-Deoxy-3-*O*- $\beta$ -D-galactopyranosyl-1-*O*-hexadecyl-2-octadecan-amido-*sn*-glycerol (13c):** obtained as a white solid from **10c**; 108 mg (79%);  $^1\text{H}$  and  $^{13}\text{C}$  NMR chemical shifts are identical with those of compound **12c**  $\pm 0.2$  and  $\pm 1.1$  ppm, respectively. Anal. Calcd for  $\text{C}_{43}\text{H}_{85}\text{NO}_8$ : C, 69.40; H, 11.51; N, 1.88. Found: C, 69.14; H, 11.57; N, 1.94.

**Evaluation of Physical Properties.** Phase identifications and determinations of phase transition temperature were carried out, concomitantly, by thermal polarized light microscopy using a Zeiss Universal polarizing transmitted light microscope equipped with a Mettler FP52 microfurnace in conjunction with an FP50 Central Processor. Photomicrographs were obtained using a Zeiss polarizing light microscope equipped with a Nikon AFM camera. Homeotropic sample preparations suitable for phase characterization were prepared simply by using very clean glass microscope slides (washed with water, acetone, water, concentrated nitric acid, water, and dry acetone). Homogeneous specimens were obtained using untreated glass slides and cover slips. Lyotropic mesophases were investigated at room temperature by placing a solid sample between a slide and a cover slip and injecting water from the side using a syringe.

Differential scanning calorimetry was used to determine enthalpies of transition and to confirm the phase transition temperatures determined by optical microscopy. Differential scanning thermograms (scan rate  $10^\circ \text{ min}^{-1}$ ) were obtained using a Perkin-Elmer DSC 7 PC system operating on DOS software. The results obtained were standardized to indium (measured onset  $156.68^\circ \text{C}$ ,  $\Delta H = 28.47 \text{ J g}^{-1}$ ; literature value  $156.60^\circ \text{C}$ ,  $\Delta H = 28.45 \text{ J g}^{-1}$ ).<sup>22</sup>

Comparison of the transition temperatures determined by optical microscopy and differential scanning calorimetry show some slight discrepancies: i.e., up to about  $3^\circ \text{C}$  in some cases. This is due to two factors: first, the two methods used separate instruments which are calibrated in different ways, and second and more importantly, the carbohydrates tended to decompose at elevated temperatures and at different rates depending on the rate of heating, the time spent at an elevated temperature, and the nature of the supporting substrate. That is, the materials decomposed more quickly in aluminum DSC pans than on glass microscope slides.

High-flux synchrotron radiation (Daresbury Laboratories, Experimental Station 8.2) was employed to investigate the structures of the mesophases by X-ray diffraction. Synchrotron radiation was used because it allows X-ray scans to be taken at a relatively fast rate as a function of temperature, thereby allowing the collection of data at elevated temperatures before appreciable degradation of the samples could occur. Samples were prepared as polycrystalline powders in Lindemann tubes maintained at a controlled temperature to allow the diffraction data to be recorded while the temperature scanning was performed at  $2^\circ \text{ min}^{-1}$  in the temperature range of  $80\text{--}180^\circ \text{C}$ . The selected experimental setup was limited to the recording of data relating to lattice constants greater than  $17.8 \text{ \AA}$ . The use of wet rat-tail collagen as a calibration standard leads to a systematic error of 3% of the observed  $d$  spacings. The wavelength of the radiation used was  $1.54 \text{ \AA}$ .

Molecular modeling studies were performed on a Silicon Graphics workstation (Indigo XS24, 4000) using QUANTA and CHARMm. Within CHARMm, the adopted basis Newton–Raphson (ABNR) algorithm was used to locate the molecular conformation with the lowest potential energy. The minimization calculations were performed until the root-mean-square (RMS) force reached  $10^{-6} \text{ kcal mol}^{-1} \text{ \AA}^{-1}$ . The RMS force is a direct measure of the tolerance applied to the energy gradient (i.e. the rate of change of potential energy with step number) during each cycle of minimization. If the average energy gradient was less than the specified value, the calculation was terminated. The modeling packages QUANTA and CHARMm assume the molecules

**Table 1.** Transition Temperatures ( $^\circ\text{C}$ ) of a Variety of Galactose Cerebrosides Derived from Bovine Brain Tissue

Naturally Occurring Galactocerebrosides from Bovine Brain I	
	R = $\text{C}_{15}\text{H}_{31}$ Crystal $146.6^\circ \text{C}$ Columnar $185.7^\circ \text{C}$ Isotropic Liquid
	R = $\text{C}_{17}\text{H}_{35}$ Crystal $91.2^\circ \text{C}$ Columnar $178.5^\circ \text{C}$ Isotropic Liquid
	R = Oleoyl Crystal $128.3^\circ \text{C}$ Columnar $176.5^\circ \text{C}$ Isotropic Liquid
	R = Nervonoyl Crystal $138.4^\circ \text{C}$ Columnar $186.6^\circ \text{C}$ Isotropic Liquid

to be a collection of hard particles held together by elastic forces, in the gas phase, at absolute zero, in an ideal motionless state. In addition to Quanta and CHARMm, molecular simulations were generated using an Apple Macintosh G3 computer and ChemDrawPro as part of the ChemDraw Ultra 6.0 program.

## Results and Discussion

**Naturally Occurring Cerebrosides I.** The selection of the steroyl, palmitoyl, oleoyl, and nervonoyl homologues of series **I** for study was driven by (i) their availability and (ii) the opportunity to compare the effects of having a double bond in both of the terminal chains versus having one of the chains being fully hydrogenated. The four naturally occurring galactocerebrosides shown in Table 1 were thus examined by thermal polarized light microscopy in their dry states. Table 1 gives the transition temperatures and mesophase classifications of the compounds in their dry (or almost dry) states. All of the materials were found to have high clearing temperatures, and thus, they exhibit relatively stable mesophases in comparison to the other series studied (see later). Interestingly, the steroyl and oleoyl members of the series have almost identical clearing points, indicating that unsaturation in at least one of the terminal aliphatic chains does not markedly affect the self-organizing properties of the materials. Conversely, the presence of a degree of unsaturation appears to raise the melting point considerably. Where the two chains are only slightly different in length,  $\pm 2$  carbon atoms, e.g. the palmitoyl derivative, higher clearing points are realized. However, the melting points are also higher, possibly due to the almost symmetrical nature of the structures of the molecules, whereas if the chains have considerably different lengths (asymmetrical) the melting points are much lower.

All of the compounds were found to exhibit hexagonal columnar phases over very wide temperature ranges. When viewed between crossed polars in the microscope ( $\times 100$ ), fanlike defects of the liquid crystal phase were readily observed

(22) *CRC Handbook of Physics and Chemistry*, 68th ed.; Priest, R. C., Ed.; CRC Press: Boca Raton, FL, 1988.



**Figure 3.** Defect texture of the columnar mesophase of *N*-palmitoyl cerebroside ( $\times 100$ ).

along with a homeotropic uniaxial defect texture (see Figure 3). In the fanlike texture no hyperbolic or elliptical lines of optical discontinuity or parabolic defects associated with focal-conic defects were observed, indicating that the mesophase could not be a lamellar/smectic phase. Conoscopy, however, was unable to determine whether the mesophase had a negative or positive birefringence; such a result could have been used to determine the direction of the optic axis. When the isotropic liquid was cooled, the mesophase separated in the form of dendrites with hexagonal symmetry, indicating that the phase has a hexagonal order. The lack of grain boundaries running across the fans also indicated that the local structure was fluid and disordered. The fanlike texture was also found to exhibit rectilinear defects, confirming that the mesophase possessed hexagonal ordering, and the lack of grain boundaries within the fans classified the phase as a columnar disordered hexagonal phase ( $Col_{hd}$ ).

Differential scanning calorimetry confirmed the results obtained by microscopy. Each of the materials showed complex melting from the solid state to the liquid crystal state, with many solid–solid transitions occurring. Typically all of the materials did not form a glassy state on cooling but instead underwent recrystallization. The lack of formation of glassy states is unusual for such liquid crystalline glycolipids, which often tend to exhibit a liquid crystal to glassy transition upon cooling with the retention of the structure of the liquid crystal phase.

In addition to exhibiting thermotropic liquid crystal phases, the materials were also found to exhibit lyotropic phases through the addition of water. Lyotropic phases suitable for microscopic studies were, however, often hard to obtain because of the poor solubilities of the materials; therefore, we resorted to mild sonication to generate suitable specimens. Figure 4 shows the texture obtained for the lyotropic phase of *N*-palmitoyl cerebroside at high water concentration. The texture of the phase was found to be very similar to that exhibited by the neat material. However, we note that as this particular material did not mix particularly well with water, segregation and precipitation occurred readily. Nevertheless, no hyperbolic and elliptical lines of optical discontinuity associated with the presence of a lamellar phase were observed. Rectilinear defects associated with columnar phases were observed, confirming the nature of the phase.

An experiment employing a water concentration gradient was also used to investigate the miscibility of the hexagonal



**Figure 4.** Defect texture of the columnar lyotropic mesophase of *N*-palmitoyl cerebroside ( $\times 100$ ).

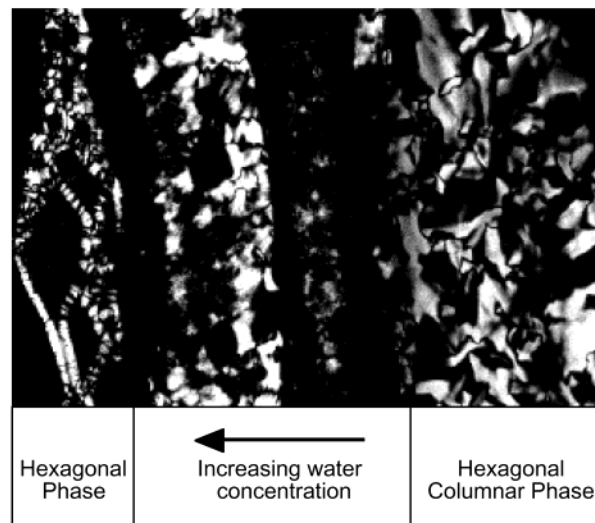
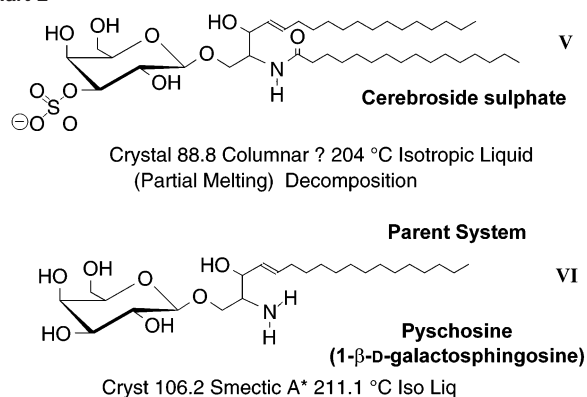


**Figure 5.** Contact preparation between water (left-hand side) and the thermotropic hexagonal phase (right-hand side) ( $\times 100$ ).

thermotropic phase with water. This experiment allowed us to investigate how the lyotropic morphology changed with change in molecular shape as the materials became solvated. Thus, water was carefully run between a microscope slide and cover slip containing a dry specimen of *N*-palmitoyl cerebroside. The slide was heated in order to generate a concentration gradient across the slide. The gradient was relatively mobile as the material partially dissolved. The microscopic texture of the concentration gradient is shown in Figure 5, with the dry specimen on the right-hand side and the high water concentration on the left-hand side of the picture. The photomicrograph shows that the hexagonal columnar thermotropic phase passes through a number of lyotropic phases as the specimen is hydrated. If the central region in Figure 5 is examined closely, it is possible to observe the formation of other phases, which probably correspond to cubic phases (black regions) and the lamellar phase (light region down the center of the photomicrograph). The presence of such phases suggests that the curvature in the system is changing as water molecules swell the headgroups of the material. Changes in the average molecular shape will thus induce different packing arrangements of the molecules, which will lead ultimately to different phases being formed. Thus, the presence of lamellar and possibly cubic phases as the concentra-

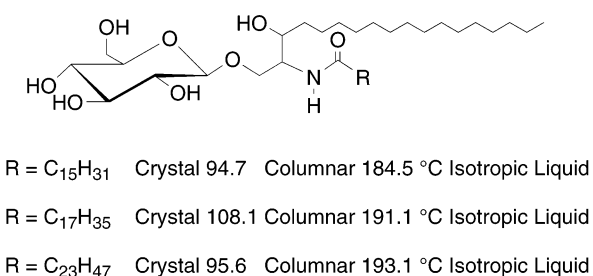


Chart 2

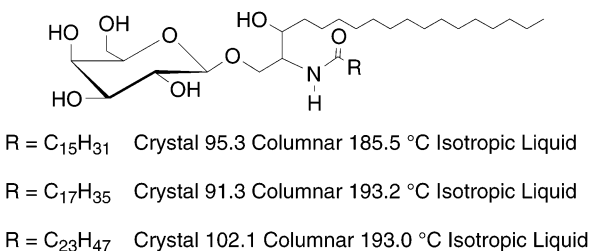


**Table 2.** Melting and Isotropization Points (°C) for the Racemic DL-Dihydro Cerebrosides II

*N*-Alkanoyl-DL-Dihydroglucocerebrosides II



*N*-Alkanoyl-DL-Dihydrogalactocerebrosides



tion changes suggests that the structures of the hexagonal lyotropic and thermotropic phases are different.

These observations lead us to conclude that the structures of the two columnar thermotropic and lyotropic liquid crystal phases are inverted with respect to one another. This outcome probably indicates that, in the columnar phase of the neat materials, the headgroups are located in the interior of the columns, whereas the reverse is the case for the lyotropic columnar phases.

To confirm the presence of thermotropic hexagonal phases, X-ray diffraction studies on the galactocerebrosides were carried out. The intensities of the reflections were, however, found to be extremely weak, even when using a synchrotron radiation source. The related material cerebroside sulfate (**V**; see Chart 2) was found by microscopy to have a hexagonal columnar phase which was miscible with the columnar phases of selected materials shown in Tables 1 and 2. Compound **V** was examined by X-ray studies and found to give a high-quality diffraction pattern, the reflections for which showed that the thermotropic liquid crystal phase is indeed a hexagonal columnar phase.

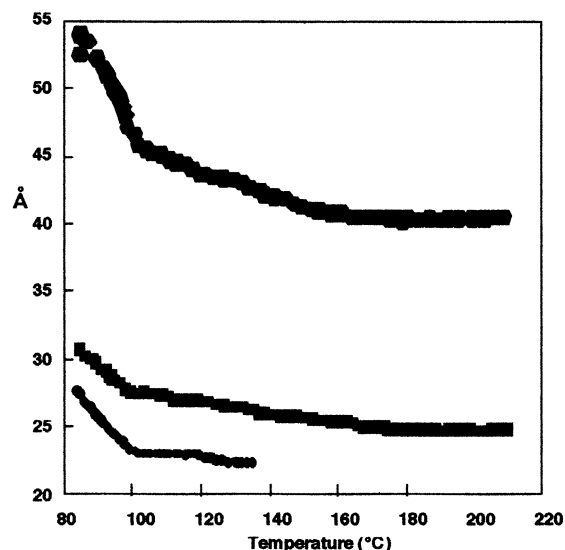


**Figure 6.** Spacings (Å) obtained by X-ray diffraction for cerebroside sulfate as a function of temperature (°C).

The reflections as a function of temperature are in the ratio of  $1:\sqrt{3}:\sqrt{4}$ , confirming the presence of a hexagonal phase (see Figure 6). As cerebroside sulfate was also found to be comiscible with materials of types **I** and **II**, this result confirms that these compounds also exhibit hexagonal columnar phases. The water concentration gradient studies by microscopy coupled with those of the X-ray investigations suggest that the structure of the thermotropic phase is one where the chains are on the outside of the columns and the carbohydrate groups are on the inside (see Figure 7 a). Thus, the chains act as an oil-like solvent, thereby producing a normal hexagonal phase where the molecules are disordered along the column axes. The texture exhibited by the lyotropic hexagonal phase coupled with the phase changes across the water concentration phase diagram suggests that the reverse is the case for the lyotropic phases, and now the swollen headgroups are on the outside and the fatty chains are on the inside of the columns as shown in Figure 7b. This result, however, does not rule out the possibility that the lyotropic phase has a bilayer structuring with headgroups on the inside and outside of the columns.

**Racemic DL-Dihydro Cerebrosides II.** As with materials of type **I**, the analogous racemic DL-dihydro cerebrobrosides **II** were also found to exhibit columnar mesophases. The melting and isotropization points are shown in Table 2 for the C<sub>15</sub>, C<sub>17</sub>, and C<sub>23</sub> chain lengths for both the galactose and analogous glucose series.

It is interesting to note that, for these materials, the melting points are much lower than those for the series **I** materials. This means that the liquid crystal phases are exhibited over much wider temperature ranges. The isotropization temperatures were found to be slightly higher with respect to compounds of type **I**, thereby indicating that the change in molecular structure on going from series **I** to **II** does not markedly affect the stability of the liquid crystalline state. Moreover, there is virtually no change in the isotropization temperature with respect to change in the sugar unit (i.e. galactose versus glucose), again demonstrating that the polar headgroup does not greatly affect the mesomorphic properties. Thus, self-organization as opposed to self-assembly in amphiphilic systems is relatively insensitive to stereochemical structure in the headgroup, which is quite

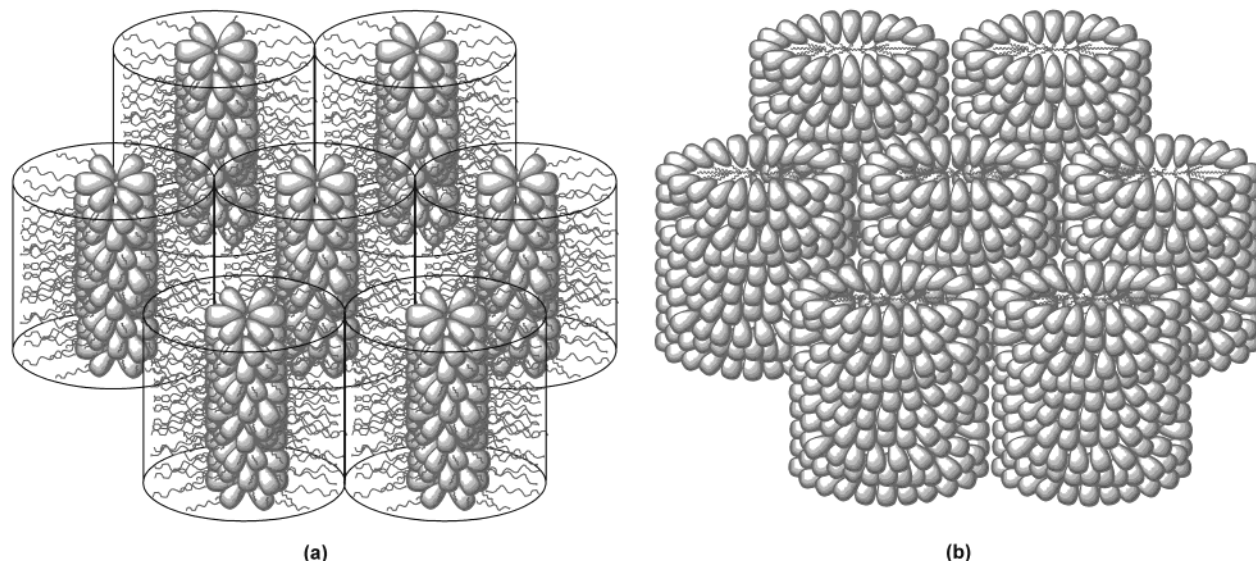


**Figure 7.** Depiction of the structure of the hexagonal columnar phase of compounds **I–III** and **V**, showing (a) the structure of the thermotropic phase and (b) the structure of the lyotropic phase.

surprising in comparison to conventional thermotropic liquid crystals, where the slightest variation in chemical structure results in large changes to the liquid crystal phase behavior. This means that these systems are ultimately very compatible and that the changes to the various structural features change secondary properties such as viscosity etc.

**Related Synthetic Glycolipids III.** Some of the synthetic glycolipids **III** (compounds **11c**, **12c**, and **13c**, **12b** and **13b**, and **11a** and **13a**), which are structurally related to the series **I** and **II**, were also found to exhibit columnar phases. The melting transitions and the isotropization points are listed for the seven new glycolipids in Table 3. However, only four of the materials are liquid crystalline; two of these (**13b** and **13c**) exhibit enantiotropic phases, whereas the other two are monotropic (**12b** and **12c**).

Interestingly, liquid crystalline phases have not been found for these materials, when one or both of the aliphatic chains are short in length. This is likely due to an unsuitable hydrophilic/hydrophobic balance in the molecular structure. Similarly, when the chains are of a similar length, mesomorphism is again suppressed in certain circumstances, e.g. **12b** and **12c**, which is probably due to a relatively symmetrical molecular structure inducing a higher melting point. For materials with long aliphatic chains attached to the amide unit, e.g.  $C_{16}$ , the transition to the solid state is reduced and the isotropization temperature is raised, leading to stabilization of the liquid crystal state. Overall the clearing points were considerably lower than those found for series **I** and **II**.

Under polarizing light microscopy the materials did not readily form homeotropic textures, and instead they gave almost entirely fanlike defect textures associated with the disordered hexagonal columnar phase (see Figure 8). The column axes were thus predominantly arranged in a disorganized way in the plane of the specimen and, therefore, perpendicular to the field of view. This organization suggests that the sugar units are not necessarily hydrogen bonding directly with the glass surfaces of the slides, which would result in the column axes being perpendicular to the glass substrates, but rather that the sugar units are not being exposed directly to the glass. A columnar



**Figure 8.** Fanlike defect texture of compound **13a** ( $\times 100$ ).

arrangement where the sugar units are located within the columns is more likely to produce a homogeneous texture, which adds more circumstantial evidence toward a model of the columnar phase in which the headgroups are located toward the center of the columns and the fatty chains are located on the outer surfaces.

The order of liquid crystal stability with respect to the three series is as follows: **II** > **I** > **III** (see Figure 9). It appears that the extra hydrogen bonding associated with the hydroxyl group in the terminal chains of **I** and **II** is in dynamic form at high temperatures in the mesophase and stabilizes mesophase formation over the ether linkage in the analogous series **III**. In particular the hydroxyl moiety in the aliphatic chain has the potential, as demonstrated through stereochemical models, to dynamically hydrogen bond with either the oxygen atom or the hydroxyl group at the 6-position in the pyranose ring (see Figure 9). Such a structure possesses a quasi-second-ring structure which would effectively raise the transition temperatures for **I** and **II** over those for the ether linked system **III**, which does not have the potential for such dynamic intramolecular hydrogen bonding. It is not clear, however, why the clearing points are lower for **I** with respect to **II**. It may be that decomposition occurs more easily for **I** than for **II**; however, the transition temperatures for the two series are perhaps too close to permit a meaningful explanation for the relative stabilities.

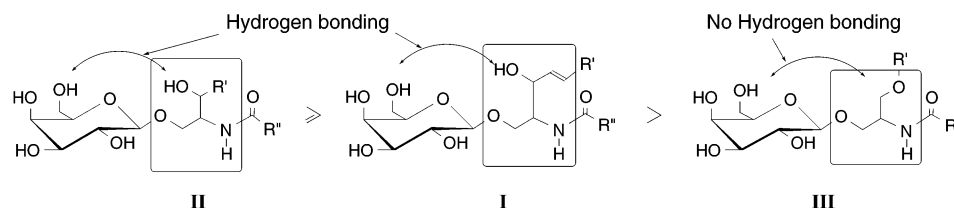


**Figure 9.** Property–structure correlations for compounds **I–III**, showing the possible locations for dynamic intramolecular hydrogen-bonding interactions.

**Table 3.** Melting and Isotropization Points (°C) for the Synthetic Glycolipids **III** (Compounds **11c–13c**, **12b** and **13b**, and **11a** and **13a**)

	<b>11c</b>
Crystal 130.8 °C Isotropic Liquid	
	<b>12c</b>
Crystal 137.5 (Columnar 132.5) °C Isotropic Liquid	
	<b>13c</b>
Crystal 134.0 Columnar 154.7 °C Isotropic Liquid	
	<b>12b</b>
Crystal 136.4 (Columnar 123.3) °C Isotropic Liquid	
	<b>13b</b>
Crystal 118.2 Columnar 132.7 °C Isotropic Liquid	
	<b>11a</b>
Crystal 115.9 °C Isotropic Liquid	
	<b>13a</b>
Crystal 119.8 °C Isotropic Liquid	

**Effect of Chirality in the Terminal Chains.** The thermotropic properties determined for diastereoisomers **IV** are shown in Table 4. It can be seen that the clearing points for the two materials are similar, indicating that the chirality associated with the attachment of one of the terminal chains is limited. Indeed, the difference in the clearing points is within experimental error in terms of the purities of the materials (liquid crystal transitions are often very sensitive to small differences in purity) and the methods of determining the clearing point temperatures: i.e. thermal microscopy and differential scanning calorimetry. The

**Table 4.** Melting and Isotropization Points (°C) for the Synthetic Glycolipids **IV**

	<b>153</b>
Crystal 153 Columnar 155.5 °C Isotropic Liquid Recryst 132.6 °C	
	<b>133.4</b>
Crystal 133.4 Columnar 151.9 °C Isotropic Liquid Recryst 94.4 °C	

melting point differences are, on the other hand, very large, as might be expected for diastereoisomers. These results demonstrate that the self-organizing liquid crystalline state is more tolerant of changes to the chirality of the system than is the solid state, or the self-assembly of molecular entities such as proteins etc.

Similar results have been found in the case of threitol- and erythritol-substituted systems, where the stereochemistry inversion occurs in the headgroup.<sup>23</sup> Again, very little difference in the isotropization temperatures occurs (within experimental error a distinction between the two diastereomers cannot be determined), which is in contrast to the melting points, which are substantially different. Thus, as with the introduction of degrees of unsaturation, changes to the stereochemistry of the system do not affect the liquid crystalline phase behavior, but large changes occur with respect to the solid state. Conversely, secondary properties, such as viscosity, might be expected to be more strongly affected.

It is also interesting to note that the parent system psychosine (**VI**; see Chart 2) exhibits a thermotropic lamellar smectic A\* phase. The formation of a lamellar phase indicates that the molecular structure is cylindrical in shape and therefore the cross-sectional area of the headgroup is similar to that of the aliphatic chain: i.e., the presence of just one terminal aliphatic chain attached to the headgroup supports the formation of smectic phases. One of the derivatives of psychosine, the galactocerebroside shown in Figure 2, has a wedge-like shape due to the presence of two aliphatic chains attached to one headgroup. When the like parts of such molecules pack together, curvature is introduced into the condensed phase. This results in the formation of thermotropic mesophases with curved structures such as columnar phases. It is interesting that when water is added, materials such as cerebroside, with one polar headgroup and two terminal aliphatic chains, have near-zero curvature due to the swelling of the headgroups by water

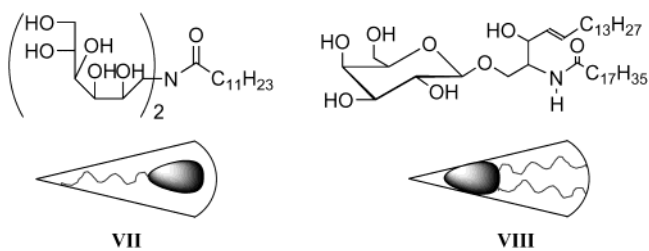
(23) Goodby, J. W.; Watson, M. J.; Mackenzie, G.; Kelly, S. M.; Bachir, S.; Bault, P.; Godé, P.; Goethals, G.; Martin, P.; Ronco, G.; Villa, P. *Liq. Cryst.* **1998**, *25*, 139.

molecules. Indeed, it appears from this work and related research<sup>24,25</sup> that thermotropic mesophases of amphiphilic materials have dependencies on the molecular shape similar to those of lyotropic liquid crystals, except that the zero curvature point is shifted for lyotropic systems toward molecular architectures possessing two chains and one headgroup. Thus, the results reported here are in keeping with those of West,<sup>24</sup> who showed that glycolipid systems with one headgroup—one chain produce a lamellar system, two headgroups—one chain and two chains—one headgroup give columnar phases, and three headgroups—one chain and three chains—one headgroup give cubic phases. In related mixture studies<sup>25</sup> between compound **VII**, which has two headgroups and one chain, and compound **VIII**, which has two chains and one headgroup (see Chart 3), the phase diagram exhibits a hexagonal columnar, cubic, lamellar, cubic, columnar hexagonal change in phase type as the concentration, and hence the curvature, is varied. The hexagonal phases were

(24) West, J. J. Ph.D. Thesis, University of Hull, 2001.

(25) West, J. J.; Bonsergent, G.; Mackenzie, G.; Ewing, D. F.; Goodby, J. W.; Benvegna, T.; Plusquellec, D.; Bachir, S.; Bault, P.; Douillet, O.; Godé, P.; Goethals, G.; Martin P.; Villa, P. *Mol. Cryst. Liq. Cryst.* **2001**, *363*, 23.

Chart 3



thus shown to have inverted structures with respect to one another. The same effects are apparent in the present study as the size of the headgroup changes with water concentration, which, in turn, influences changes in the curvature and mesophase type.

**Acknowledgment.** We thank M.-N. Bouchu and J. A. Haley for technical assistance and the Centre National de la Recherche Scientifique and the Alliance Programme of the British Council and the Ministère des Affaires Étrangères, Direction de la Coopération Scientifique et Technique for financial support.

JA020396+